Manuscript prepared for Geosci. Model Dev.
with version 2015/04/24 7.83 Copernicus papers of the LaTeX class copernicus.cls.
Date: 28 July 2015

Impact of ocean coupling strategy on high-resolution global atmosphere simulations

Colin M. Zarzycki[1], Kevin A. Reed[2], Julio Bacmeister[1], Susan C. Bates[1], Anthony P. Craig[1], and Nan A. Rosenbloom[1]

[1]Climate and Global Dynamics, National Center for Atmospheric Research, Boulder, Colorado, USA.
[2]School of Marine and Atmospheric Sciences, State University of New York at Stony Brook, Stony Brook, New York, USA.

Correspondence to: Colin M. Zarzycki, Climate and Global Dynamics, National Center for Atmospheric Research, Boulder, Colorado, USA. (zarzycki@ucar.edu)

Abstract. The abstract goes here.

1 Introduction

The use of general circulation models (GCMs) to evaluate global tropical cyclone (TC) characteristics in current and future climate has grown considerably over the last decade. It has been shown that GCMs can model TCs at horizontal resolutions of approximately 100 km grid spacing with limitations (e.g., Bengtsson et al., 2007; Knutson et al., 2010; Strachan et al., 2013). As models have advanced to even higher horizontal resolutions (i.e., ≤ 50 km) the simulated climatology of tropical cyclones has improved greatly (e.g., Oouchi et al., 2006; Zhao et al., 2009; Murakami et al., 2012; Manganello et al., 2012; Satoh et al., 2012; Bacmeister et al., 2014; Wehner et al., 2014; Reed et al., 2015). Furthermore, the use of variable-resolution GCMs have shown to be useful for the study of regional TC climatologies at reduced computational cost compared to equivalent global high-resolution simulations, providing further resources capable of pushing climate simulations to finer grid spacings (Zarzycki et al., 2014a; Zarzycki and Jablonowski, 2014).

Recently, intercomparisons have shown that the range of simulated TC climatology across different climate models can be large (Camargo, 2013; Walsh et al., 2015). It has also been shown that within individual GCMs TC characteristics can vary greatly depending on model design choices. Various studies have documented the large uncertainty in TC simulations due to the choice of individual subgrid parameterizations, such as cumulus parameterizations (e.g., Kim et al., 2012; Reed and Jablonowski, 2011a; Lim et al., 2014)), while others have focused on differences due to changes in whole parameterization suites (Reed and Jablonowski, 2011b; Bacmeister et al., 2014). The dynamical core, the main fluid flow component of a GCM, has also been shown to be an important source of uncertainty for TC simulations, though less widely documented (Reed and Jablonowski, 2012; Zhao et al., 2012; Reed et al., 2015).

In this manuscript we describe another mechanism through which simulated TC properties are influenced by model design choices, in particular, the manner in which the ocean and atmosphere are coupled within the climate system. In particular, we will utilize the Community Atmosphere Model 5 (CAM5), within the Community Earth System Model (CESM), to explore the impact of two different strategies for coupling to a prescribed ocean. CAM5 has shown increasing ability to model tropical cyclones at high horizontal resolutions of 0.25° (Bacmeister et al., 2014; Wehner et al., 2014; Wehner et al., 2015; Reed et al., 2015) and a similar model setup will be used for part of this study.

The reminder of the paper is organized as follows. Section 2 provides an introduction to the modeling system used in this study and how coupling between the atmosphere and ocean is treated. Section 3 investigates the impact on multi-year climate simulations while Section 4 details the sensitivity of TCs to the ocean grid using a deterministic forecast framework while. Section 5 discusses the results and offers further insight into their implications.

2 Model description

2.1 Community Earth System Model

In this paper, we utilize CESM which is a community climate model which allows for atmospheric simulations to be coupled to land, ocean, and ice models (Hurrell et al., 2013). The atmospheric component CAM5 (Neale et al., 2010) is configured with the Spectral Element (SE) dynamical core. SE is the newest dynamical core available in CAM5 and is based upon continuous Galerkin spectral finite elements which are applied on a cubed-sphere grid (Taylor et al., 1997; Thomas and Loft, 2005; Taylor and Fournier, 2010). In addition to attractive conservation properties (Taylor, 2011), CAM-SE has shown appealing scaling properties since atmospheric primitive equations are solved locally on individual elements (Dennis et al., 2012; Evans et al., 2013). The land model is the Community Land Model (CLM) version 4.0 run in satellite phenology (SP) mode (Oleson et al., 2010). While CESM also allows for coupling to dynamic ocean and ice models, all of the simulations here utilize prescribed SSTs and ice cover concentrations. In the default CESM configuration, prescribed SSTs and ice are passed to the model on a 1°x1° grid and internally interpolated to the ocean and ice grids.

2.2 Coupling within CESM

When all earth system model components operate on identical grids, vertical coupling (such as between the ocean surface and lowest level of the atmosphere) is straightforward. However, since these components are generally not integrated on the same spatial grid, CPL7 is used to couple these components to one another within the CESM framework (Craig et al., 2012). The coupler utilizes remapping weights to regrid quantities which are needed across model components. Figure 1 provides a schematic of the coupling process when differences exist between, for example, the resolution of

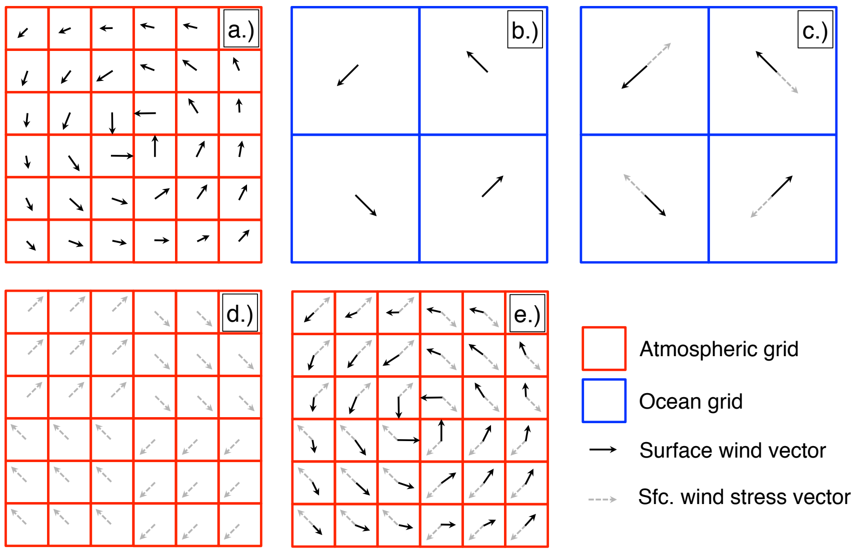

Figure 1. Coupling procedure in CESM. Red (blue) boxes indicate atmospheric (ocean) grid cells. Black (Gray) solid (dashed) vectors show surface wind (wind stress) vectors.

the atmosphere and ocean grids in CESM. In this case, the atmospheric grid (red) is of finer resolution. This is the default setup for many climate configurations in CESM, in particular, configurations which use prescribed SSTs and ice data for forcing.

Atmospheric variables, such as winds (black vectors; taken here to approximate the flow associated with a tropical cyclone), are computed on the atmospheric grid (Fig. 1a). When coupling is required, these values are then conservatively remapped to the ocean grid (blue) (Fig. 1b). Surface momentum stress (τ, gray vectors) and sensible and latent heat fluxes are calculated on the ocean grid using these remapped values (Fig. 1c). The calculated quantities are then remapped back to the atmospheric grid using either conservative remapping or bilinear interpolation (Fig. 1d), where they are used by the atmospheric component of the model for integration (Fig. 1e).

3 Climate simulations

We first compare TC statistics in two multi-decadal climate simulations using 0.25° (~28km, denoted as ne120 on the spectral element cubed sphere grid) resolution for the atmosphere. Both simulations follow Atmospheric Model Intercomparison Project (AMIP) protocols (Gates, 1992) and are coupled to CLM with an equivalent grid resolution of 0.25°. The first simulation is coupled to a prescribed ocean/ice model using a grid where the polar point is displaced over Greenland, which is at approximately 1° horizontal resolution (ne120_gx1v6). This is coarser than both the atmosphere and land models. The second simulation is identical to the first except the prescribed ocean/ice model operates on the same 0.25° grid as the atmosphere and land (ne120_ne120). For both simulations, all quantities calculated by coupling the atmosphere and ocean/ice are carried out on the ocean grid. These are both supported grid configurations in CESM. It is worth nothing that while the ocean/ice model operates on the 0.25° grid, the data is interpolated from the same 1.0° observational dataset used in the first simulation. SSTs and ice coverage are applied using the monthly 1° Hadley Centre Sea Ice and Sea Surface Temperature dataset (HadISST, Hurrell et al. (2008)).

Both simulations are integrated from 1980 to 2005. Taylor statistics for the 1980-1999 global-mean quantities for sea-level pressure (PSL), total precipitable water (TMQ), total precipitation rate (PRECT), 200 hPa zonal wind (U200), 850 hPa zonal wind (U850), 600 hPa relative humidity (RH600) and 500 hPa temperature (T500) are shown in Fig. 2. The two simulations are compared to observational datasets including NCEP (Kalnay et al., 1996) (PSL, U200, U850, RH600, T500), MERRA (Rienecker et al., 2011) (TMQ), and TRMM (Huffman et al., 2007) (PRECT). The absolute distance from the origin (lower left) represents the magnitude of the spatial variability within the domain (as measured by normalized standard deviation) while the spatial correlation is plotted as the radial angle between the model marker and the origin. A comprehensive discussion of Taylor diagram analysis can be found in Taylor (2001). Red dots highlight the climatology of the ne120_ne120 simulation while blue dots show the same for the ne120_gx1v6 simulation. This analysis is only concerned with the relative difference between the two simulations and, therefore, whether or not mean climatology is impacted by choice of coupling grid. A thorough analysis understanding why each parameter is modeled with their particular skill in CAM5 itself is beyond the scope of this paper. We do note, however, that the results are generally consistent with skill scores reported in previous CAM5 modeling studies, such as Bacmeister et al. (2014) (their Fig. 2 and Fig. 3) and Zarzycki et al. (2015) (their Fig. 9).

The most notable result from assessing this skill is the two simulations are highly similar in a global climatological sense. All markers in the ne120_gx1v6 simulation overlap with their corresponding variable from the ne120_ne120 simulation. The occurrence of this overlap highlights that the mean climate state is not impacted by choice of coupling strategy in the climate simulations.

While the mean climatology of the two simulations are essentially identical, notable differences arise when comparing TC statistics between the two simulations. TCs are objectively tracked in model output using the method first outlined in Vitart et al. (1997) and updated by Knutson et al. (2007). The version of the TC tracker applied in this study utilizes 3-hourly model output and is described in detail in Zhao et al. (2009). Previous work using this technique to find TCs in CAM/CESM output have produced a realistic storm climatology both spatially and in terms of storm intensity Reed et al. (2015). For the tracker, all data is regridded from the CAM-SE cubed sphere to a 0.25° latitude-longitude grid as in Reed et al. (2015). Surface winds (commonly taken to be at a height of 10 m) are approximated from the lowermost model level winds ($\approx$ 60 m) and a logarithmic law similar to the approach described in Zarzycki and Jablonowski (2014).

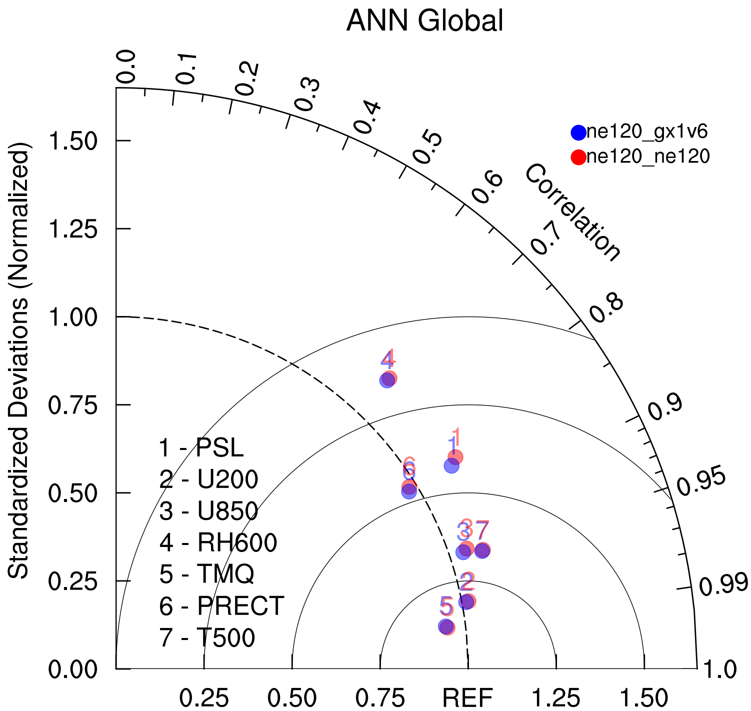

Figure 2. Taylor diagram for globally- and annually-averaged climate statistics. Blue circles represent the results from AMIP simulation coupled to 1° ocean grid (ne120_gx1v6) and red circles represent the same for simulation using 0.25° ocean grid (ne120_ne120). See text for description of the diagram and explanation of acronyms.

Table 1. Annual frequency of global tropical cyclones that reach tropical storm (cat. 0-5), hurricane (cat. 1-5) and major hurricane (cat. 4-5) strength the CAM5 simulations and IBTrACS observations for the time period of 1980 to 2005.

Simulation	**Total Storms**	**Hurricanes**	**Major Hurricanes**
IBTrACS	91.6 ± 8.5	47.1 ± 5.5	10.7 ± 3.3
ne120_gx1v6	70.1 ± 9.0	55.5 ± 7.7	12.5 ± 3.4
ne120_ne120	73.2 ± 10.5	50.3 ± 8.2	4.2 ± 1.9

Table 1 displays storm counts for all TCs, storms that reach hurricane strength and storms that reach major hurricane strength on the Saffir-Simpson scale (Simpson, 1974) (defined here as categories 4 and 5) for each simulation for 1980 through 2005. Observations from the International Best Track Archive for Climate Stewardship (IBTrACS, Knapp et al. (2010)) for the same time period are provided as a reference. Both simulations produce roughly the same frequency of total storms. However, the simulation coupled to the lower resolution ocean produces 10% more hurricanes and nearly three times the amount of major hurricanes when compared to the simulation with the higher resolution coupling. This signifies a shift towards high intensities in the ne120_gx1v6 configuration.

To explore this further, Figure 3 displays the minimum surface pressure vs. maximum wind speed relationship for tropical cyclones for each simulation with a quadratic least squares fit shown as a solid line. IBTrACS observations are again included as a reference and to be consistent with the TC tracker only storms that reach tropical storm strength in their lifetime are used. At low wind speeds (i.e., <40 m/s) the relationship between the minimum surface pressure and maximum wind speed for the two model simulations and observations compare well. However, at larger wind speeds the relationship between the two simulations diverges consistent to the differences in TC counts in Table 1. In particular, the ne120_gx1v6 simulation produces greater winds speeds at a given minimum pressure than ne120_ne120 simulation, suggesting the ocean coupling resolution impact on tropical cyclone intensity is non-negligible.

Figure 4 shows the number of annual 60-m wind exceedances in the 3-hourly model output for both category 4 and category 5 storm thresholds. These represent the two most intense classifications of tropical cyclones, with maximum sustained winds surpassing 59 m s^{-1} and 70 m s^{-1}, respectively. While these are wind thresholds associated with intense TCs they are calculated over the entire ocean domain from 30°S to 30°N and are therefore not necessarily only representative of TCs in the model (CMZ - we can drop this qualification (which I feel is preferable) if Julio confirms that these extremes are associated with TCs, which I assume is the case). The bolder, black curve indicates the number of data points surpassing each threshold for the simulation using the 1° ocean/ice grid (ne120_gx1v6) while the red curve marked by crosses represents the same for the simulation with the 0.25° ocean/ice grid (ne120_ne120). From the left panel, we see that for all years (except 1985), the simulations coupled to the coarser ocean grid produces a significantly greater frequency of category 4 level winds. This behavior is even more pronounced in the right panel, where the ne120_gx1v6 simulation averages approximately 5 instances of category 5 level winds per year. However, this threshold is not exceeded at any point during the 26-year sample in the ne120_ne120 simulation.

4 Deterministic simulations

Since all aspects of the model configurations in the climate simulations are identical except for the grid on which the prescribed SSTs and ice concentrations are passed to the other model components,

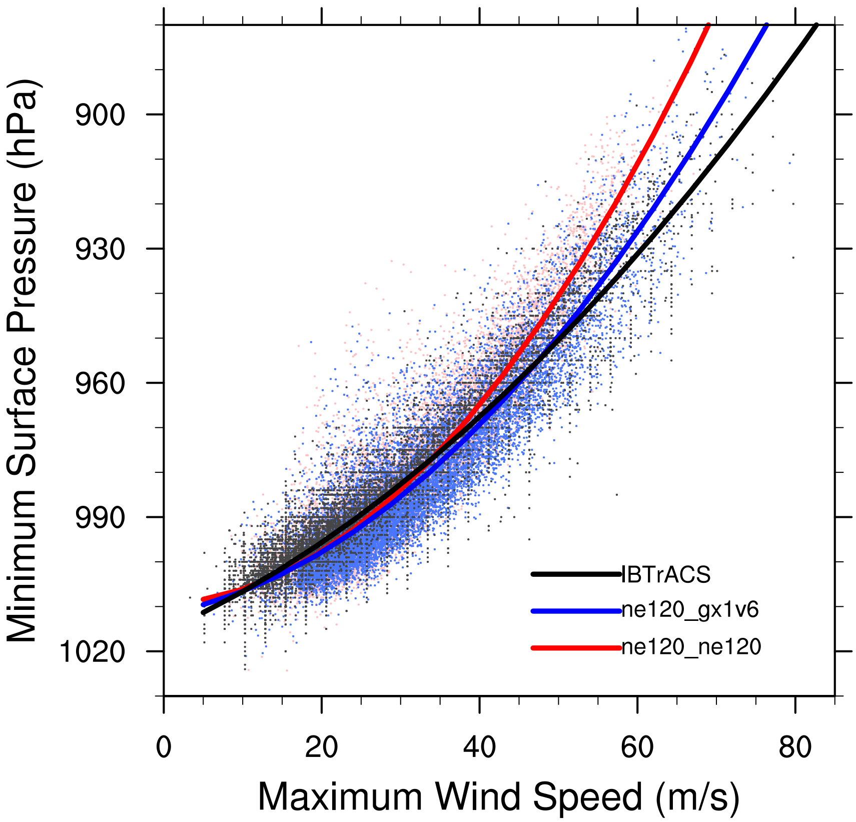

Figure 3. Storm minimum surface pressure vs. maximum wind speed relationship with quadratic least squares fit (solid lines) for the CAM5 simulations and IBTrACS observations from 1980 to 2005. Note that 3-hourly output is used for the model simulations, while the IBTrACS data is 6-hourly.

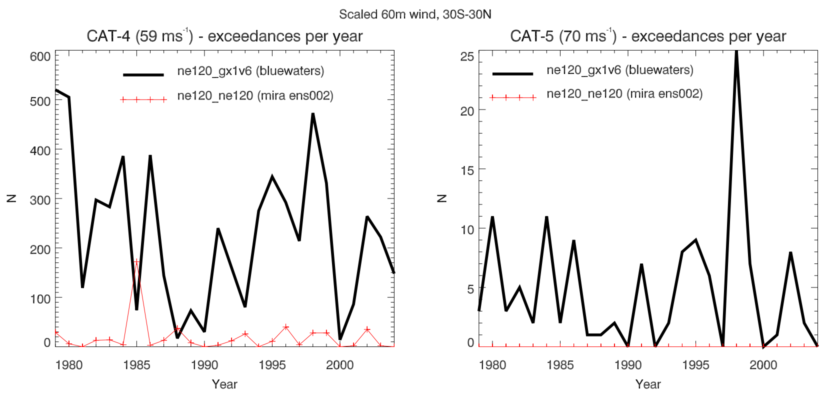

Figure 4. Number of TC surface wind instances exceeding category 4 and category 5 wind thresholds for AMIP simulation coupled to 1° ocean grid (ne120_gx1v6) and 0.25° ocean grid (ne120_ne120). Instances are calculated using 3-hourly data.

we hypothesize that the marked difference in TC climatology is induced by the coupling strategy and difference in grid resolutions. To assess the differences in simulated TCs in a controlled, deterministic manner, we utilize two identical CAM setups to complete short-term forecast simulations of observed storms. These simulations utilize the new, variable-resolution capability of CAM-SE (Zarzycki et al., 2014b).

The setup is similar to that used in the previous section, but the model is configured with a variable-resolution atmospheric grid with 0.125° (~14km, ne240) resolution over the Atlantic Ocean. Forecast simulations are initialized with a digitally-filtered atmospheric analysis from the National Center for Atmospheric Predictions's Global Data Assimilation System (GDAS). Observed SSTs on a 1°x1° grid are derived from the NOAA High-resolution Blended Analysis (Reynolds et al., 2007). The land surface is modeled by CLM 4.0 is initialized with a state nudged to be in balance with the atmospheric initial conditions. The model setup and initialization are both further detailed in Zarzycki and Jablonowski (2015).

As in the climate simulations, the only difference between the two setups is the grid used by the data ocean and ice models. The first set of simulations uses the aforementioned displaced pole grid with an equivalent resolution of 1° (ne240_gx1v6) while the second uses an ocean grid identical to the atmospheric grid with an equivalent resolution of 0.125° (ne240_ne240). Since the SST and ice cover data are provided at coarser scales than the model interpolates to, any differences in the results arise due to the differences in calculating of surface fluxes and momentum drag on the corresponding ocean grids.

After initialization, each configuration is integrated for 8 days. Figure 5 shows the 120-hour forecasts for Hurricane Leslie in the North Atlantic Ocean from the 2012 hurricane season. The simulation was initialized at 00Z on August 31st, 2012 making Fig. 5 valid at 00Z on September 5th, 2012. The forecast using the 1° ocean grid with default coupling configuration (calculations done on ocean grid) is on the left (Fig. 5a,d), with the 0.125° ocean grid in the center (Fig. 5b,e). All fields are extracted from the atmospheric model component. The top panels depict instantaneous lowest model level wind (black vectors) as well as the surface frictional stress vector (red).

In Fig. 5a, it is readily apparent that many instances exist where the vectors are not aligned. This results from the surface stress being calculated on the coarser grid. The atmospheric dynamical core then subsamples this coarser information to provide stress information at the same resolution used by the numerics (as in Fig. 1). In Fig. 5b, the wind and stress vectors are parallel (180° difference), indicating that the frictional drag is acting in direct opposition to the wind within the atmospheric dynamical core, which is the expected behavior from theory. The higher resolution ocean grid preserves the resolution of the surface wind field during stress calculations. Because of this, not only are the stress vectors properly aligned with the high-resolution ocean grid, the maximum magnitudes of the stress vectors are larger at the storm's radius of maximum wind in Fig. 5b. This highlights that maxima in the stress field at the atmospheric grid cell scale are preserved with the higher resolution

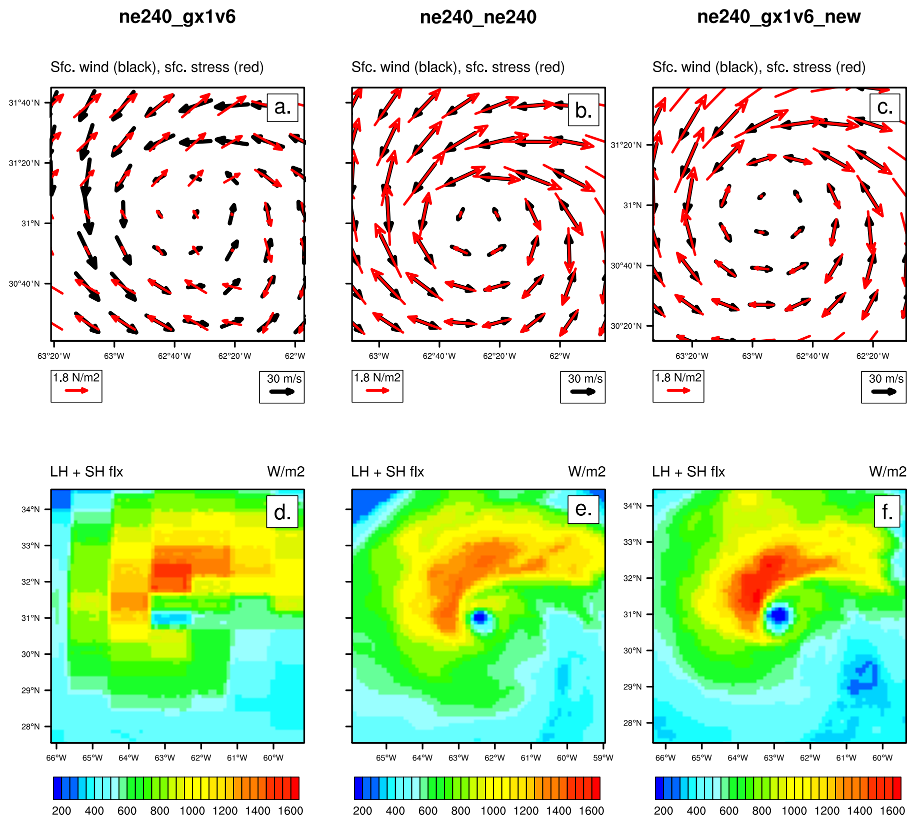

Figure 5. 120-hour CAM-SE forecast for Hurricane Leslie, valid at 00Z on September 5th, 2012. Left panels (a,d) are results from forecast using 1° ocean grid in the default configuration (calculations carried out on ocean grid). Center panels (b,e) show results using 0.125° ocean grid. Right panels show version of 1° grid where calculations are carried out on the atmospheric grid. Top panels (a-c) display instantaneous wind in the lowest model (black vectors) with corresponding lowest model level wind stress (red vectors). Lower panels (d-f) show total surface flux (latent plus sensible heat).

ocean grid, whereas these maxima are "smoothed" in the calculation where wind is first averaged to the coarser ocean grid (Fig. 5a), leading to disparate forcing on wind speeds when passed back to the atmospheric model. This is further evidenced by the fact that the integrated dot product (over a 5°x5° domain centered over the TC minimum surface pressure) of the two fields is approximately 10% smaller in the simulations using the 1° ocean grid. Therefore, the use of the coarser ocean grid results in a universally weaker frictional force fed back to the atmospheric dynamics, leading to enhanced extreme wind speeds.

The cumulative surface heat flux is shown on the bottom (sensible plus latent) for the two storms at the same forecast time. It is readily apparent that the coarser ocean grid (Fig. 5d) provides information back to the atmosphere with significantly less spatial structure than the 0.125° ocean grid (Fig. 5e). While the difference in 5°x5° integrated heat flux is relatively small (approximately 1%), it is clear that the spatial structure of the heat flux field is very different between the two model configurations. This may further play a role in storm dynamics, with the 1° ocean grid providing a larger, more diffuse source of surface heating to the TC core than the high-resolution grid.

To conclusively verify that this discrepancy arises from the choice of coupling, we complete a third simulation, which is identical to the ne240_gx1v6 simulation, except coupling calculations are carried out on the higher-resolution atmospheric grid (ne240_gx1v6_reverse). If the TC behavior in the ne240_gx1v6 configuration is due to errors arising from carrying out computations on the coarser grid in the coupling system, we expect this to be primarily alleviated by ensuring coupling is carried out on the higher-resolution grid. This should thereby result in maximum spatial resolution of the computed fields and no 'loss' of information due to interpolation from fine to coarse and back to fine resolutions. Figures 5c,f show the same analysis as the previous configurations. It is apparent that inverting the grid to ensure calculations of surface stresses and fluxes are done on the higher resolution grid (in this case, the atmosphere) results in a solution that looks much more similar to the configuration where both atmosphere and ocean are of high-resolution (Figs. 5b,e). Examples of these similarities include the fact that surface stresses are stronger and aligned parallel to lowest model level wind vectors as well as added fine scale structure in the total surface flux field.

5 Conclusions

This manuscript describes biases in atmospheric extreme climatology which arise from choice of ocean grid and coupling strategy in CESM. Since surface stress and flux calculations are carried out on the ocean grid, running the model with a coarser ocean than atmosphere presents problems with respect to tropical cyclone (TC) climatology. In particular, surface stress vectors which are passed back to the atmospheric dynamical core following coupling are not aligned with the surface wind due to being computed on a coarser grid. This allows winds near the core of TCs to become stronger than if the stresses were computed at the same resolution of the atmosphere. Additionally, when surface fluxes are calculated on a different grid, the influx of heat and moisture to the lowest levels of the atmosphere underneath the TC are structurally different, with these quantities being more diffuse and misaligned with the maximum surface wind, in contradiction to bulk aerodynamical flux theory.

The issues outlined in the manuscript underscore that the choice of ocean grid when using SST and ice data to force a dynamic atmosphere is not trivial, even if this forcing data is of relatively coarse resolution. However, they are easy to correct for these configurations, particularly since applying coupled atmosphere-ocean calculations on the same grid is straightforward and computationally 'cheap.'

More problematic adjustments may arise when coupling to a dynamical ocean model. The vast majority of coupled, dynamic simulations not only utilize differing resolutions between different model components, but also different numerical techniques and grids. Therefore, remapping between components is, in many cases, an absolute necessity. The obvious recommendation to alleviate coupling inconsistencies when it is not feasible to use identical grids is to calculate these quantities on the finest resolution grid of the coupled system. Performing coupling in this manner ensures that information passed back to a model component has not be interpolated to a resolution coarser than the component's native resolution during the coupling process. In addition, in integrated models which allow for multiple grid options, the choice of the model component defining the grid for these calculations should not be pre-configured for all cases, but rather, determined dynamically based on the resolutions chosen for the particular model setup.

However, we emphasize that, even when using this suggestion, it is not clear that it is fully appropriate for coupled dynamical models to be run at highly disparate resolutions from one another, where processes interacting between components may be sufficiently non-linear that merely averaging from a higher resolution grid is not the most appropriate mechanism. Further work will be required to determine whether or not this is the case. Additionally, this strategy is not elementary when multi-resolution grids are coupled to uniform grids, particularly where the finest and coarsest scales of the multi-resolution grid may straddle the uniform resolution. In these cases, the choice of 'finer' grid in the atmosphere-ocean coupling will be different depending on the region of interest, and may require a more flexible framework.

Our results demonstrate that the mean climatology of the simulations presented here are essentially identical regardless of coupling strategy, highlighting that this impact only becomes readily apparent in the tail of the distributions of interest. However, with climate models being used more and more frequently for direct analysis of TCs, as well as other extreme events, both in present climate and under future scenarios, this impact on model-derived extremes may become more prevalent. This is especially relevant as models continue to march forward with respect to horizontal resolution, and therefore, their ability to dynamically resolve atmospheric phenomena at smaller and smaller spatial scales. Consideration of these impacts when utilizing high-resolution climate data for analysis is required and modifications to how the current generation of atmospheric models treats coupling between various earth system components may be necessary.

Acknowledgements. The National Center for Atmospheric Research is sponsored by the National Science Foundation. The authors would like to thank John E. Truesdale for assistance in performing the simulations. Resources of the Argonne Leadership Computing Facility at Argonne National Laboratory, which is supported by the Office of Science of the U.S. Department of Energy under contract DE-AC02-06CH11357, were used for this research. Furthermore, this work utilizes part of the "Using Petascale Computing Capabilities to Address Climate Change Uncertainties" PRAC allocation support by the National Science Foundation ACI-1036146. This work is also part of the Blue Waters sustained-petascale computing project, which is supported by the National Science Foundation (awards OCI-0725070 and ACI-1238993) and the state of Illinois. Blue Waters is a joint effort of the University of Illinois at Urbana-Champaign and its National Center for Supercomputing Applications. Bacmeister was partially supported through the Scientific Discovery through Advanced Computing (SciDAC) program funded by U.S. Department of Energy, Office of Science, Advanced

Scientific Computing Research. Bates was supported by the Regional and Global Climate Modeling Program (RGCM) of the US. Department of Energy, Office of Science (BER), Cooperative Agreement DE-FC02-97ER62402. IBTrACS data were freely obtained from the National Oceanic and Atmospheric Administration (http://www.ncdc.noaa.gov/ibtracs/). Model data from all simulations in this manuscript are archived and available at NCAR upon request through the authors.

References

Bacmeister, J. T., Wehner, M. F., Neale, R. B., Gettelman, A., Hannay, C., Lauritzen,, P. H., Caron, J. M., and Truesdale, J. E.: Exploratory High-Resolution Climate Simulations using the Community Atmosphere Model (CAM), J. Climate, 27, 3073–3099, doi:10.1175/JCLI-D-13-00387.1, 2014.

Bengtsson, L., Hodges, K. I., and Esch, M.: Tropical cyclones in a T159 resolution global climate model: comparison with observations and re-analyses, Tellus A, 59, 396–416, doi:10.1111/j.1600-0870.2007.00236.x, 2007.

Camargo, S. J.: Global and Regional Aspects of Tropical Cyclone Activity in the CMIP5 Models, J. Climate, 26, 9880–9902, doi:10.1175/JCLI-D-12-00549.1, 2013.

Craig, A. P., Vertenstein, M., and Jacob, R.: A new flexible coupler for earth system modeling developed for CCSM4 and CESM1, Int. J. High Perf. Comput. Appl., 26, 31–42, doi:10.1177/1094342011428141, 2012.

Dennis, J. M., Edwards, J., Evans, K. J., Guba, O., Lauritzen, P. H., Mirin, A. A., St-Cyr, A., Taylor, M. A., and Worley, P. H.: CAM-SE: A scalable spectral element dynamical core for the Community Atmosphere Model, Int. J. High Perf. Comput. Appl., 26, 74–89, doi:10.1177/1094342011428142, 2012.

Evans, K. J., Lauritzen, P. H., Mishra, S. K., Neale, R. B., Taylor, M. A., and Tribbia, J. J.: AMIP Simulation with the CAM4 Spectral Element Dynamical Core, J. Climate, 26, 689–709, doi:10.1175/JCLI-D-11-00448.1, 2013.

Gates, W. L.: AMIP: The Atmospheric Model Intercomparison Project, Bull. Amer. Meteor. Soc., 73, 1962–1970, 1992.

Huffman, G. J., Adler, R. F., Bolvin, D. T., Gu, G., Nelkin, E. J., Bowman, K. P., Hong, Y., Stocker, E. F., and Wolff, D. B.: The TRMM Multisatellite Precipitation Analysis (TMPA): Quasi-global, multiyear, combined-sensor precipitation estimates at fine scales., J. Hydrometeorol., 8, 2007.

Hurrell, J. W., Hack, J. J., Shea, D., Caron, J. M., and Rosinski, J.: A New Sea Surface Temperature and Sea Ice Boundary Dataset for the Community Atmosphere Model, Journal of Climate, 21, 5145–5153, doi:10.1175/2008JCLI2292.1, 2008.

Hurrell, J. W., Holland, M. M., Gent, P. R., Ghan, S., Kay, J. E., Kushner, P. J., Lamarque, J. F., Large, W. G., Lawrence, D., Lindsay, K., Lipscomb, W. H., Long, M. C., Mahowald, N., Marsh, D. R., Neale, R. B., Rasch, P., Vavrus, S., Vertenstein, M., Bader, D., Collins, W. D., Hack, J. J., Kiehl, J., and Marshall, S.: The Community Earth System Model: A Framework for Collaborative Research, Bull. Amer. Meteor. Soc., 94, 1339–1360, doi:10.1175/BAMS-D-12-00121.1, 2013.

Kalnay, E., Kanamitsu, M., Kistler, R., Collins, W., Deaven, D., Gandin, L., Iredell, M., Saha, S., White, G., Woollen, J., Zhu, Y., Leetmaa, A., Reynolds, R., Chelliah, M., Ebisuzaki, W., Higgins, W., Janowiak, J., Mo, K. C., Ropelewski, C., Wang, J., Jenne, R., and Joseph, D.: The NCEP/NCAR 40-Year Reanalysis Project, Bull. Amer. Meteor. Soc., 77, 437–471, doi:10.1175/1520-0477(1996)077<0437:TNYRP>2.0.CO;2, 1996.

Kim, D., Sobel, A. H., Del Genio, A. D., Chen, Y., Camargo, S. J., Yao, M.-S., Kelley, M., and Nazarenko, L.: The Tropical Subseasonal Variability Simulated in the NASA GISS General Circulation Model, J. Climate, 25, 4641–4659, doi:10.1175/JCLI-D-11-00447.1, 2012.

Knapp, K. R., Kruk, M. C., Levinson, D. H., Diamond, H. J., and Neumann, C. J.: The International Best Track Archive for Climate Stewardship (IBTrACS), Bull. Amer. Meteor. Soc., 91, 363–376, doi:10.1175/2009BAMS2755.1, 2010.

Knutson, T. R., Sirutis, J. J., Garner, S. T., Held, I. M., and Tuleya, R. E.: Simulation of the Recent Multidecadal Increase of Atlantic Hurricane Activity Using an 18-km-Grid Regional Model, Bull. Amer. Meteor. Soc., 88, 1549, doi:10.1175/BAMS-88-10-1549, 2007.

Knutson, T. R., McBride, J. L., Chan, J., Emanuel, K., Holland, G., Landsea, C., Held, I., Kossin, J. P., Srivastava, A. K., and Sugi, M.: Tropical cyclones and climate change, Nature Geosci., 3, 157–163, doi:10.1038/ngeo779, 2010.

Lim, Y.-K., Schubert, S. D., Reale, O., Lee, M.-I., Molod, A. M., and Suarez, M. J.: Sensitivity of Tropical Cyclones to Parameterized Convection in the NASA GEOS-5 Model, J. Climate, 28, 551–573, doi:10.1175/JCLI-D-14-00104.1, 2014.

Manganello, J. V., Hodges, K. I., Kinter, J. L., Cash, B. A., Marx, L., Jung, T., Achuthavarier, D., Adams, J. M., Altshuler, E. L., Huang, B., Jin, E. K., Stan, C., Towers, P., and Wedi, N.: Tropical Cyclone Climatology in a 10-km Global Atmospheric GCM: Toward Weather-Resolving Climate Modeling, J. Climate, 25, 3867–3893, doi:10.1175/JCLI-D-11-00346.1, 2012.

Murakami, H., Wang, Y., Yoshimura, H., Mizuta, R., Sugi, M., Shindo, E., Adachi, Y., Yukimoto, S., Hosaka, M., Kusunoki, S., Ose, T., and Kitoh, A.: Future Changes in Tropical Cyclone Activity Projected by the New High-Resolution MRI-AGCM, J. Climate, 25, 3237–3260, doi:10.1175/JCLI-D-11-00415.1, 2012.

Neale, R. B., Chen, C.-C., Gettelman, A., Lauritzen, P. H., Park, S., Williamson, D. L., Conley, A. J., Garcia, R., Kinnison, D., Lamarque, J.-F., Marsh, D., Mills, M., Smith, A. K., Tilmes, S., Vitt, F., Cameron-Smith, P., Collins, W. D., Iacono, M. J., , Easter, R. C., Liu, X., Ghan, S. J., Rasch, P. J., and Taylor, M. A.: Description of the NCAR Community Atmosphere Model (CAM 5.0), NCAR Technical Note NCAR/TN-486+STR, National Center for Atmospheric Research, Boulder, Colorado, 2010.

Oleson, K., Lawrence, D., Bonan, G., Flanner, M., Kluzek, E., Lawrence, P., Levis, S., Swenson, S., Thornton, P., Dai, A., Decker, M., Dickinson, R., Feddema, J., Heald, C., Hoffman, F., Lamarque, J., Mahowald, N., Niu, G., Qian, T., Randerson, J., Running, S., Sakaguchi, K., Slater, A., Stockli, R., Wang, A., Yang, Z., Zeng, X., and Zeng, X.: Technical Description of version 4.0 of the Community Land Model (CLM), NCAR Technical Note NCAR/TN-478+STR, National Center for Atmospheric Research, Boulder, Colorado, doi:10.5065/D6FB50WZ, 2010.

Oouchi, K., Yoshimura, J., Yoshimura, H., Mizuta, R., Kusunoki, S., and Noda, A.: Tropical Cyclone Climatology in a Global-Warming Climate as Simulated in a 20 km-Mesh Global Atmospheric Model: Frequency and Wind Intensity Analyses, J. Meteorol. Soc. Jpn.,, 84, 259–276, 2006.

Reed, K. A. and Jablonowski, C.: Impact of physical parameterizations on idealized tropical cyclones in the Community Atmosphere Model, Geophys. Res. Lett., 38, doi:10.1029/2010GL046297, 2011a.

Reed, K. A. and Jablonowski, C.: Assessing the Uncertainty of Tropical Cyclone Simulations in NCAR's Community Atmosphere Model, J. Adv. Model. Earth Syst., 3, M08 002, doi:10.1029/2011MS000076, 2011b.

Reed, K. A. and Jablonowski, C.: Idealized tropical cyclone simulations of intermediate complexity: A test case for AGCMs, J. Adv. Model. Earth Syst., 4, M04 001, doi:10.1029/2011MS000099, 2012.

Reed, K. A., Bacmeister, J. T., Wehner, Rosenbloom, N. A., F., M., Bates, S. C., Lauritzen, P. H., Truesdale, J. T., and Hannay, C.: Impact of the dynamical core on the direct simulation of tropical cyclones in a high-resolution global model, Geophys. Res. Lett., 42, doi:10.1002/2015GL063974, in press, 2015.

Reynolds, R. W., Smith, T. M., Liu, C., Chelton, D. B., Casey, K. S., and Schlax, M. G.: Daily High-Resolution-Blended Analyses for Sea Surface Temperature, Journal of Climate, 20, 5473–5496, doi:10.1175/2007JCLI1824.1, 2007.

Rienecker, M. M., Suarez, M. J., Gelaro, R., Todling, R., Bacmeister, J., Liu, E., Bosilovich, M. G., Schubert, S. D., Takacs, L., Kim, G.-K., Bloom, S., Chen, J., Collins, D., Conaty, A., da Silva, A., Gu, W., Joiner, J., Koster, R. D., Lucchesi, R., Molod, A., Owens, T., Pawson, S., Pegion, P., Redder, C. R., Reichle, R., Robertson, F. R., Ruddick, A. G., Sienkiewicz, M., and Woollen, J.: MERRA: NASA's Modern-Era Retrospective Analysis for Research and Applications, J. Climate, 24, 3624–3648, doi:10.1175/JCLI-D-11-00015.1, 2011.

Satoh, M., Oouchi, K., Nasuno, T., Taniguchi, H., Yamada, Y., Tomita, H., Kodama, C., Kinter, J., Achuthavarier, D., Manganello, J., Cash, B., Jung, T., Palmer, T., and Wedi, N.: The Intra-Seasonal Oscillation and its control of tropical cyclones simulated by high-resolution global atmospheric models, Climate Dynamics, 39, 2185–2206, doi:10.1007/s00382-011-1235-6, 2012.

Simpson, R. H.: The Hurricane Disaster – Potential Scale, Weatherwise, 27, 169–186, doi:10.1080/00431672.1974.9931702, 1974.

Strachan, J., Vidale, P. L., Hodges, K., Roberts, M., and Demory, M.-E.: Investigating Global Tropical Cyclone Activity with a Hierarchy of AGCMs: The Role of Model Resolution, J. Climate, 26, 133–152, doi:10.1175/JCLI-D-12-00012.1, 2013.

Taylor, K. E.: Summarizing multiple aspects of model performance in a single diagram, J. Geophys. Res.-Atmos, 106, 7183–7192, doi:10.1029/2000JD900719, 2001.

Taylor, M., Tribbia, J., and Iskandarani, M.: The Spectral Element Method for the Shallow Water Equations on the Sphere, J. Comput. Phys., 130, 92–108, 1997.

Taylor, M. A.: Conservation of Mass and Energy for the Moist Atmospheric Primitive Equations on Unstructured Grids, in: Numerical Techniques for Global Atmospheric Models, edited by Lauritzen, P. H., Jablonowski, C., Taylor, M. A., and Nair, R. D., vol. 80 of *Lecture Notes in Computational Science and Engineering*, pp. 357–380, Springer, 2011.

Taylor, M. A. and Fournier, A.: A compatible and conservative spectral element method on unstructured grids, J. Comput. Phys., 229, 5879–5895, 2010.

Thomas, S. and Loft, R.: The NCAR Spectral Element Climate Dynamical Core: Semi-Implicit Eulerian Formulation, J. Sci. Comput., 25, 307–322, doi:10.1007/s10915-004-4646-2, 2005.

Vitart, F., Anderson, J. L., and Stern, W. F.: Simulation of interannual variability of tropical storm frequency in an ensemble of GCM integrations, J. Climate, 10, 745–760, 1997.

Walsh, K. J. E., Camargo, S. J., Vecchi, G. A., Daloz, A. S., Elsner, J., Emanuel, K., Horn, M., Lim, Y.-K., Roberts, M., Patricola, C., Scoccimarro, E., Sobel, A. H., Strazzo, S., Villarini, G., Wehner, M., Zhao, M., Kossin, J. P., LaRow, T., Oouchi, K., Schubert, S., Wang, H., Bacmeister, J., Chang, P., Chauvin, F., Jablonowski, C., Kumar, A., Murakami, H., Ose, T., Reed, K. A., Saravanan, R., Yamada, Y., Zarzycki, C. M., Vidale, P. L., Jonas, J. A., and Henderson, N.: Hurricanes and climate: the U.S. CLIVAR working group on hurricanes, Bull. Amer. Meteor. Soc., doi:10.1175/BAMS-D-13-00242.1, 2015.

Wehner, M. F., Reed, K. A., Li, F., Prabhat, Bacmeister, J., Chen, C.-T., Paciorek, C., Gleckler, P. J., Sperber, K. R., Collins, W. D., Gettelman, A., and Jablonowski, C.: The effect of horizontal resolution on simulation quality in the Community Atmospheric Model, CAM5.1, J. Adv. Model. Earth Syst., doi:10.1002/2013MS000276, 2014.

Wehner, M. F., Prabhat, Reed, K. A., Stone, D., Collins, W. D., and Bacmeister, J. T.: Resolution dependence of future tropical cyclone projections of CAM5.1 in the US CLIVAR Hurricane Working Group idealized configurations, J. Climate, 28, 3905–3925, doi:10.1175/JCLI-D-14-00311.1, 2015.

Zarzycki, C. M. and Jablonowski, C.: A multidecadal simulation of Atlantic tropical cyclones using a variable-resolution global atmospheric general circulation model, J. Adv. Model. Earth Syst., 6, 805–828, doi:10.1002/2014MS000352, 2014.

Zarzycki, C. M. and Jablonowski, C.: Experimental tropical cyclone forecasts using a variable-resolution global model, Mon. Wea. Rev., in prep., 2015.

Zarzycki, C. M., Jablonowski, C., and Taylor, M. A.: Using Variable Resolution Meshes to Model Tropical Cyclones in the Community Atmosphere Model, Mon. Wea. Rev., 142, 1221–1239, doi:10.1175/MWR-D-13-00179.1, 2014a.

Zarzycki, C. M., Levy, M. N., Jablonowski, C., Overfelt, J. R., Taylor, M. A., and Ullrich, P. A.: Aquaplanet Experiments Using CAM's Variable-Resolution Dynamical Core, J. Climate, 27, 5481–5503, doi:10.1175/JCLI-D-14-00004.1, 2014b.

Zarzycki, C. M., Jablonowski, C., Thatcher, D. R., and Taylor, M. A.: Effects of localized grid refinement on the general circulation and climatology in the Community Atmosphere Model, J. Climate, 28, 2777—2803, doi:10.1175/JCLI-D-14-00599.1, 2015.

Zhao, M., Held, I. M., Lin, S. J., and Vecchi, G. A.: Simulations of Global Hurricane Climatology, Interannual Variability, and Response to Global Warming Using a 50-km Resolution GCM, J. Climate, 22, 6653–6678, 2009.

Zhao, M., Held, I. M., and Lin, S.-J.: Some Counterintuitive Dependencies of Tropical Cyclone Frequency on Parameters in a GCM, J. Atmos. Sci., 69, 2272–2283, doi:10.1175/JAS-D-11-0238.1, 2012.